Neuron, Vol. 34, 387–397, April 25, 2002, Copyright ©2002 by Cell Press

PSD-95 Mediates Formation of a Functional Homomeric Kir5.1 Channel in the Brain

Masayuki Tanemoto, Akikazu Fujita, Kayoko Higashi, and Yoshihisa Kurachi[1]
Department of Pharmacology II
Graduate School of Medicine A7
Osaka University
Yamada-oka 2-2
Suita, Osaka 565-0871
Japan

Summary

Homomeric assembly of Kir5.1, an inward-rectifying K^+ channel subunit, is believed to be nonfunctional, although the subunit exists abundantly in the brain. We show that HEK293T cells cotransfected with Kir5.1 and PSD-95 exhibit a Ba^{2+}-sensitive inward-rectifying K^+ current. Kir5.1 coexpressed with PSD-95 located on the plasma membrane in a clustered manner, while the Kir5.1 subunit expressed alone distributed mostly in cytoplasm, probably due to rapid internalization. The binding of Kir5.1 with PSD-95 was prevented by protein kinase A (PKA)-mediated phosphorylation of its carboxyl terminus. The currents flowing through Kir5.1/PSD-95 were suppressed promptly and reversibly by PKA activation. Because the Kir5.1/PSD-95 complex was detected in the brain, this functional brain K^+ channel is potentially a novel physiological target of PKA-mediated signaling.

Introduction

Inwardly rectifying K^+ (Kir) channels play pivotal roles in controlling the excitability of various cells, including neurons. The Kir channel subunit family contains more than 16 members, which can be classified into four major groups: background Kir channels (Kir2.0), G protein-gated Kir channels (Kir3.0), ATP-sensitive Kir channels (Kir6.0), and K^+ transporters (Kir1.0/4.0) (Isomoto et al., 1997; Jan and Jan, 1997). Kir5.1 is a unique subunit that does not belong to these major groups. While Kir5.1 was reported to form no functional channel when expressed alone in heterologous expression systems (Bond et al., 1994; Pessia et al., 1996), it can coassemble with members of Kir4.0 and modulate their channel properties (Pessia et al., 1996; Pearson et al., 1999). It was recently proposed that a heteromeric K^+ channel composed of Kir5.1 and Kir4.1 may physiologically function as a proton sensor in kidney (Tanemoto et al., 2000; Tucker et al., 2000; Xu et al., 2000). However, we found that most Kir5.1 protein expressed in brain did not coassemble with Kir4.1 (Tanemoto et al., 2000). Therefore, an unidentified mechanism might be required to allow the formation of functional homomeric Kir5.1 channels in situ.

We noticed that Kir5.1 possesses an amino acid sequence, SQM, at its carboxyl (C) end. This sequence corresponds to a motif for interaction with PDZ domains, PSD-95/Dlg/ZO-1 (also known as discs-large homology repeats or GLGF repeats), of anchoring proteins (Craven and Bredt, 1998; Sheng 2001). In brain, a family of anchoring proteins named membrane associated guanylate kinases (MAGUKs), such as PSD-95/SAP90, SAP97, and PSD-93/Chapsin-110, are highly expressed (Craven and Bredt, 1998). These MAGUKs contain several PDZ, one SH3, and one guanylate kinase (GK) domain. They, especially PSD-95, are enriched at the postsynaptic density (PSD) of excitatory synapses (Cho et al., 1992). In this study, we detected a complex of Kir5.1 and PSD-95 in brain. Therefore, it seemed possible that the Kir5.1/PSD-95 complex might exist in the PSD of excitatory synapses and play some functional roles. To evaluate this possibility, we examined the effects of PSD-95 on the function and intracellular distribution of the Kir5.1 channel in HEK293T cells. We found that HEK293T cells cotransfected with Kir5.1 and PSD-95 exhibited Ba^{2+}-sensitive K^+ currents. While Kir5.1 expressed alone distributed mostly in cytoplasm, probably due to rapid internalization, Kir5.1 coexpressed with PSD-95 located on plasma membrane in a clustered manner. The binding of these proteins required three C-terminal amino acids (SQM) of Kir5.1 and the region from PDZ3 to SH3 of PSD-95. PKA-mediated phosphorylation of Kir5.1 disrupted the binding. Furthermore, PKA activation rapidly and reversibly suppressed the current flowing through the Kir5.1/PSD-95 complex prior to the internalization of channels. Therefore, the Kir5.1/PSD-95 channel at PSD is potentially a novel target of PKA-mediated signaling systems.

Results

Homomeric Assembly of Kir5.1 Coexpressed with PSD-95 Forms a Functional K^+ Channel

HEK293T cells transfected with either Kir5.1 or PSD-95 alone exhibited no K^+ current ($n = 15$ for each). When cells were transfected with both Kir5.1 and PSD-95, inwardly rectifying K^+ currents were detected in more than half of the cells examined (8/15 cells) (Figures 1A and 1B). The expressed K^+ current was completely blocked by 3 mM Ba^{2+}. The Ba^{2+}-sensitive K^+ current was -57.2 ± 4.6 pA/pF at -100 mV with $[K^+]_o$ of 140 mM (mean ± SE, $n = 8$). The slope conductance of expressed current increased as $[K^+]_o$ was raised (Figure 1C). The reversal potential of the expressed current exhibited 57.8 mV alteration per 10-fold change in $[K^+]_o$ (Figure 1D). This was nearly identical to the theoretical value for perfectly K^+-selective channels. Therefore PSD-95 aided Kir5.1 in forming a functional homomeric K^+ channel in HEK293T cells.

A significant amount of Kir5.1 is expressed in brain as well as in kidney (Tanemoto et al., 2000). Therefore, we examined whether immunoprecipitants with anti-Kir5.1 antibody obtained from these organs contained PSD-95 or SAP97. Although both MAGUKs could be detected from brain by Western blot analysis, the immunoprecipitant obtained from brain with anti-Kir5.1 anti-

[1]Correspondence: ykurachi@pharma2.med.osaka-u.ac.jp

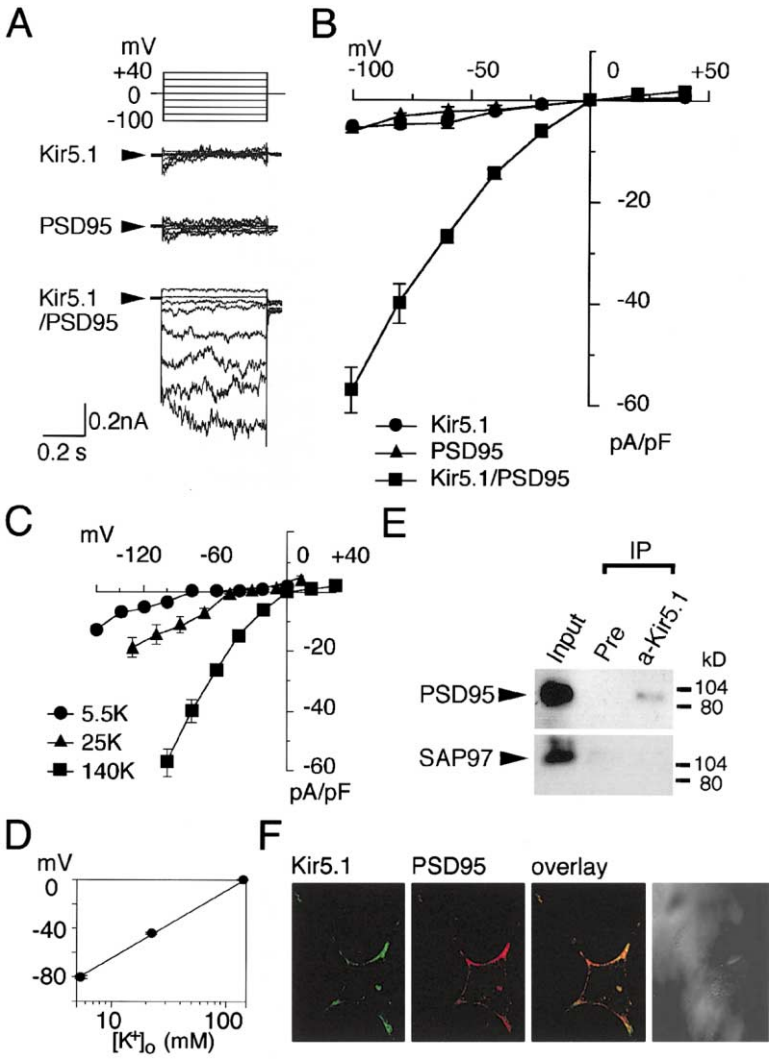

Figure 1. Functional K^+ Channel Formation by Kir5.1 and PSD-95 in HEK293T Cells and Evidence for Existence of the Kir5.1/PSD-95 Complex in Brain

(A) Representative whole-cell currents recorded from HEK293T cells expressing GFP-Kir5.1 (Kir5.1) or PSD-95 (PSD-95) alone, and coexpressing GFP-Kir5.1 and PSD-95 (Kir5.1/PSD-95), as indicated. Both pipette and bath solutions contain 140 mM K^+. Voltage steps were delivered from a holding potential of 0 mV to potentials between −100 mV and +40 mV in +20 mV increments. Traces show current records obtained following subtraction of the Ba^{2+}-insensitive component. Arrowheads indicate 0 current level.

(B) Whole-cell current-voltage relationships of cells expressing Kir5.1 (circles, n = 3), PSD-95 (triangles, n = 3), and Kir5.1/PSD-95 (squares, n = 8). Currents were measured at the end of command pulses and were normalized to cell surface capacitance. Data are shown as means ± SE.

(C) Whole-cell current-voltage relationships of Kir5.1/PSD-95 currents in different extracellular K^+ concentrations ($[K^+]_o$). Current is normalized to cell capacitance. Circles, triangles, and squares show current-voltage relationships in $[K^+]_o$ of 5.5, 25, and 140 mM, respectively. Data are shown as means ± SE (n = 3).

(D) Reversal potentials of Kir5.1/PSD-95 currents plotted against the logarithmic value of $[K^+]_o$. The line represents the Nernstian relation for a K^+ selective current.

(E) The existence of the Kir5.1/PSD-95 complex in brain lysate of rat brain was confirmed by immunoprecipitation with preimmune control IgG (Pre) or anti-Kir5.1 antibody (a-Kir5.1) as indicated. Lysate of brain was loaded as a control (Input). PSD-95, but not SAP97, was specifically coimmunoprecipitated by anti-Kir5.1.

(F) Colocalization of Kir5.1 with PSD-95 in primary cultured cerebral neuron. Primary cultured cerebral neuron (day 7) from rat embryo (E17–E18) was subjected to anti-Kir5.1 antibody (green) and anti-PSD-95 antibody (red). Kir5.1 colocalizes with PSD-95 in somato-dendritic regions in a clustered manner, as shown by yellow signals in overlay.

body contained only PSD-95 (Figure 1E). Furthermore, in cultured neurons obtained from rat brain cortex, Kir5.1 immunoreactivity was detected in a clustered manner at the somato-dendritic regions where PSD-95 immunoreactivity was also localized (Figure 1F). In kidney, on the other hand, neither PSD-95 nor SAP97 was detected by Western blot analysis, and the immunoprecipitant obtained with anti-Kir5.1 antibody did not contain either MAGUK. These results suggest that PSD-95 and Kir5.1 actually form a protein complex in vivo in brain.

PSD-95 Alters Intracellular Location of Kir5.1

To identify mechanisms responsible for Kir5.1 channel activation by PSD-95, we examined the effect of PSD-95 on the intracellular distribution of Kir5.1 in HEK293T cells (Figure 2). When expressed alone, the fluorescence of GFP-tagged wild-type Kir5.1 (GFP-Kir5.1) distributed diffusely in cytoplasm (Figure 2A). These cells exhibited no K^+ current, as shown in Figure 1A. When coexpressed with PSD-95, GFP-Kir5.1 distributed in a clustered manner on or near the plasma membrane in about 10% of cells (Figure 2B). In these cells, PSD-95 colocated with GFP-Kir5.1, as indicated by the prominent yellow signals produced in overlaid views (right panels in Figure 2B). The remaining cells in which GFP-Kir5.1 distributed diffusely were not stained with anti-PSD-95 antibody (data not shown).

The distribution of Kir5.1 was further examined with immunoelectron microscopy (Figure 2C). When expressed alone, the immunoreactivity for GFP tagged to Kir5.1 was detected in cytoplasm, while it was associated with the plasma membrane when coexpressed with PSD-95 (white arrows in the middle panel of Figure 2C). The graph in Figure 2C summarizes the density of gold particles in the area within 30 nm adjacent to plasma membrane. While in the cells transfected with GFP-Kir5.1 alone, few particles were detected in the vicinity of plasma membrane (1.50 ± 0.49/μm, n = 3), a significantly larger number of particles (16.64 ± 0.96/μm, n = 3) located near the plasma membrane when cotransfected with PSD-95.

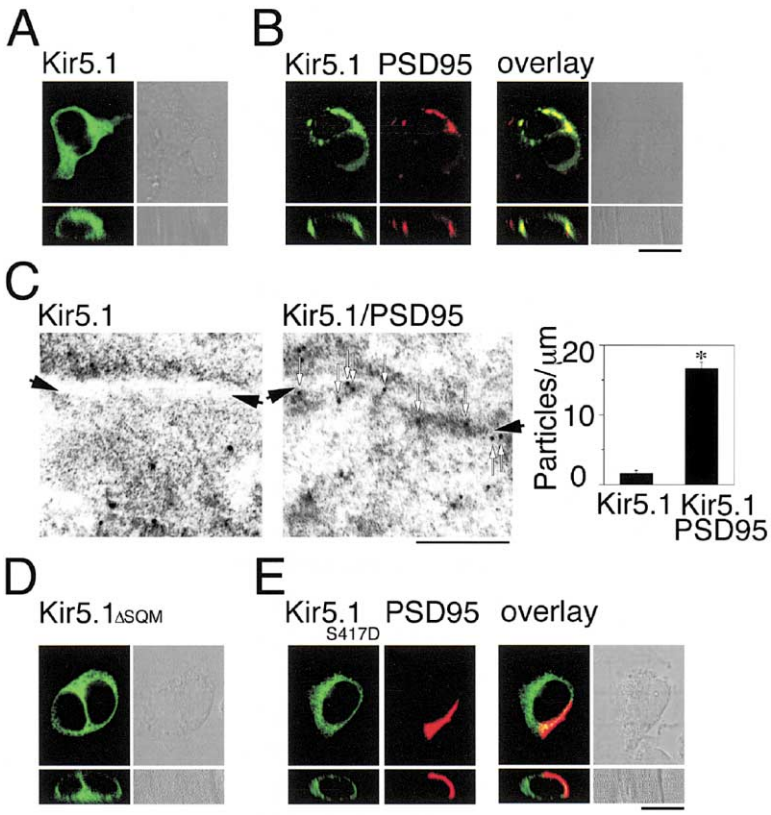

Figure 2. Clustering and Cell Surface Expression of Kir5.1 by PSD-95

(A and B) Location of GFP-Kir5.1 (green) and PSD-95 (red) in HEK293T cells. The upper and lower panels show top and side views of cells. Kir5.1 expressed alone was located diffusely in cytoplasm (A). When coexpressed with PSD-95, Kir5.1 showed a clustered distribution adjacent to the cell surface (B). PSD-95 colocated with Kir5.1, as shown by yellow signals in overlay. Scale bar: 10 μm.

(C) Immunogold electron microscopic observation of GFP-Kir5.1 in HEK293T cells. Immunopositive gold particles were detected only in the cytoplasm of Kir5.1-alone-expressed cells (Kir5.1). In Kir5.1/PSD-95-coexpressed cells, particles were detected close to the cell surface (indicated by white arrows; Kir5.1/PSD95). Black arrows indicate the cell surface membrane. Scale bar: 300 nm. The right graph illustrates the number of particles within 30 nm of the cell surface. Particles were counted, normalized to the unit length of plasma membrane, and represented in each column (means ± SE from three different regions). Asterisk indicates statistical significance between Kir5.1 and Kir5.1/PSD-95 ($p < 0.05$).

(D and E) Location of Kir5.1ΔSQM and Kir5.1S417D. Kir5.1ΔSQM (D) and Kir5.1S417D (E) diffusely located in the cytoplasm, did not cluster, and did not colocate with PSD-95 even when coexpressed with PSD-95. Scale bar: 10 μm.

Kir5.1 possesses a putative PDZ binding motif at its C terminus. A deletion mutant (Kir5.1ΔSQM) and a point mutant, in which serine 417 was mutated to aspartate (Kir5.1S417D), distributed diffusely in cytoplasm even in the presence of PSD-95 (Figures 2D and 2E). In these cells, PSD-95 did not colocate with these mutants (Figure 2E). These results suggest that the C-terminal PDZ binding motif is indispensable for Kir5.1 to interact with PSD-95.

Domains Responsible for Kir5.1/PSD-95 Interaction

To confirm that the C-terminal PDZ binding motif is required for Kir5.1 to interact with PSD-95, we performed GST pull-down studies using the C-terminal 58 amino acid segment (CT58) of Kir5.1 (Figure 3A). PSD-95 bound to this segment of wild-type Kir5.1, but not to that of a deletion mutant (ΔSQM) or that of a point mutant (S417D). These results were consistent with the diffuse cytosolic distribution of Kir5.1ΔSQM and Kir5.1S417D even in the presence of PSD-95 (Figures 2D and 2E). It was also confirmed that no functional K^+ current was detected in the HEK293T cells cotransfected with Kir5.1S417D and wild-type PSD-95 ($n = 5$; upper traces in Figure 3C).

To identify the regions in PSD-95 that interact with Kir5.1, we performed GST pull-down studies against GFP-Kir5.1 using several domains of PSD-95 (Figure 3B). The right panel of Figure 3B shows the designs of various deletion mutants of PSD-95. While all of the GST fusion proteins that contained the region from PDZ3 to SH3 of PSD-95 (PDZ3-SH3) could bind to Kir5.1, those that lacked either PDZ3 or SH3 could not. The cells cotransfected with PDZ3-SH3 and Kir5.1, however, did not express any significant K^+ current ($n = 5$; lower traces in Figure 3C). Therefore, PDZ3-SH3 is necessary and sufficient for PSD-95 to interact with Kir5.1, but not enough to aid Kir5.1 in forming a functional K^+ channel. Domains in PSD-95 other than PDZ3-SH3 may play an indispensable but as yet unidentified role in forming a functional Kir5.1 channel.

PSD-95 Increases Cell Surface Expression of Kir5.1

We next examined the effect of PSD-95 on the distribution of Kir5.1 proteins in membrane and vesicle fractions of HEK293T cells (Figure 4A). For comparison, the distribution of Kir4.1, which forms a functional K^+ channel by itself, was also examined. When expressed alone, Kir5.1 was mostly detected in the vesicle fraction, while Kir4.1 was detected equally in membrane and vesicle fractions. We calculated in each case the relative content of channel proteins in the membrane fraction with reference to that in the vesicle fraction by using NIH image software (right graph in Figure 4A). The relative content of Kir5.1 was 0.30 ± 0.04 ($n = 3$), which was significantly lower than that of Kir4.1 (1.17 ± 0.22, $n = 3$). When PSD-95 was coexpressed, the amount of Kir5.1 in the membrane fraction increased, and the relative membrane content became 0.76 ± 0.08 ($n = 3$). The relative membrane content of a mutant, Kir5.1S417D, which did not bind to PSD-95, was 0.29 ± 0.06 ($n = 3$), even with coexpression of PSD-95. The value was similar to that of wild-type Kir5.1 expressed alone. Similar re-

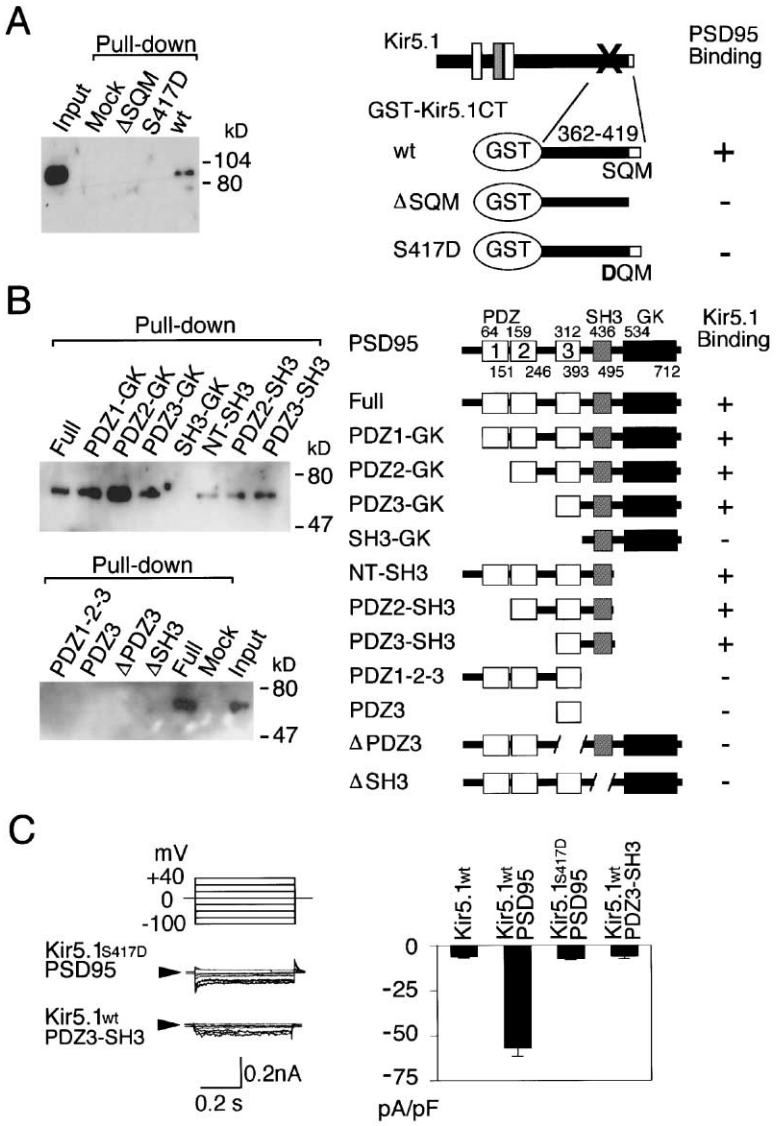

Figure 3. Domains of Interaction between Kir5.1 and PSD-95

(A) PSD-95 binding domain on Kir5.1. Constructs of GST-tagged Kir5.1 C-terminal segments are shown in the right scheme. The wild-type Kir5.1 C terminus, but neither deletion mutant (ΔSQM) nor point mutant (S417D), coprecipitated PSD-95. The cell lysate used for immunoprecipitation was loaded to indicate the correct size of PSD-95 (Input).

(B) Kir5.1 binding domain on PSD-95. Constructs of different regions of PSD-95 tagged to GST are shown on the right. Any GST fusion constructs containing the region from PDZ3 to SH3, but no construct lacking either PDZ3 or SH3, could coprecipitate GFP-Kir5.1. The cell lysate used for immunoprecipitation was loaded to indicate the correct size of GFP-Kir5.1 (Input).

(C) Representative whole-cell currents recorded from HEK293T cells expressing GFP-Kir5.1S417D/full-length PSD-95 (Kir5.1S417D/PSD95) and GFP-Kir5.1/PDZ3-SH3 of PSD-95 (Kir5.1wt/PDZ3-SH3). Whole-cell currents were recorded as described in Figure 1A. Arrowheads indicate 0 current level. The bar graph summarizes currents at −100 mV (means ± SE; n = 5).

sults were also obtained in the case of Kir5.1ΔSQM (n = 3; data not shown).

We also examined the distribution of a deletion mutant, Kir5.1Δ49, in which the C-terminal 49 amino acids that contain a putative endoplasmic reticulum (ER) retention signal motif, RRR, were deleted. The signal (RKR) at the corresponding portion in Kir6.0 has been shown to cause ER retention of this subunit (Zerangue et al., 1999). The relative content of Kir5.1Δ49 in membrane fraction was 0.27 ± 0.08 (n = 3), which was similar to that of wild-type Kir5.1 expressed alone. This result suggests that the putative ER retention signal is not responsible for the distribution of Kir5.1 in the vesicle fraction.

In Figure 4B, we performed further cell surface biotinylation studies, where only the proteins that are exposed to extracellular space are expected to be biotinylated. We performed these experiments at room temperature (22–24°C) and also at 4°C. At room temperature, synthesis and sorting of proteins would take place continuously, while they would be largely disturbed at 4°C. Thus, at room temperature, any proteins that are exposed to extracellular space even transiently during the incubation period could be biotinylated. On the other hand, at 4°C, only the proteins that are stably expressed on the cell surface during the biotinylation procedure could be biotinylated.

At room temperature, both Kir4.1 and Kir5.1 were biotinylated, even when expressed alone. In contrast, at 4°C, while a relatively large amount of Kir4.1 was biotinylated, little Kir5.1 was biotinylated. When PSD-95 was coexpressed, the amount of biotinylated Kir5.1 at 4°C increased prominently. In each case, the amount of Kir5.1 was normalized with reference to that of Kir4.1 for comparison (right graph in Figure 4B). Coexpression of PSD-95 did not alter the content of Kir5.1 expressed in HEK293T cells (0.98 ± 0.07 for Kir5.1 and 0.97 ± 0.05 for Kir5.1/PSD-95, n = 3 for each). At room temperature, the amount of biotinylated Kir5.1 was 1.25 ± 0.05 (n = 3) when expressed alone and 0.95 ± 0.04 (n = 3) when coexpressed with PSD-95. Thus coexpression of PSD-95 did not increase the amount of Kir5.1 reaching the

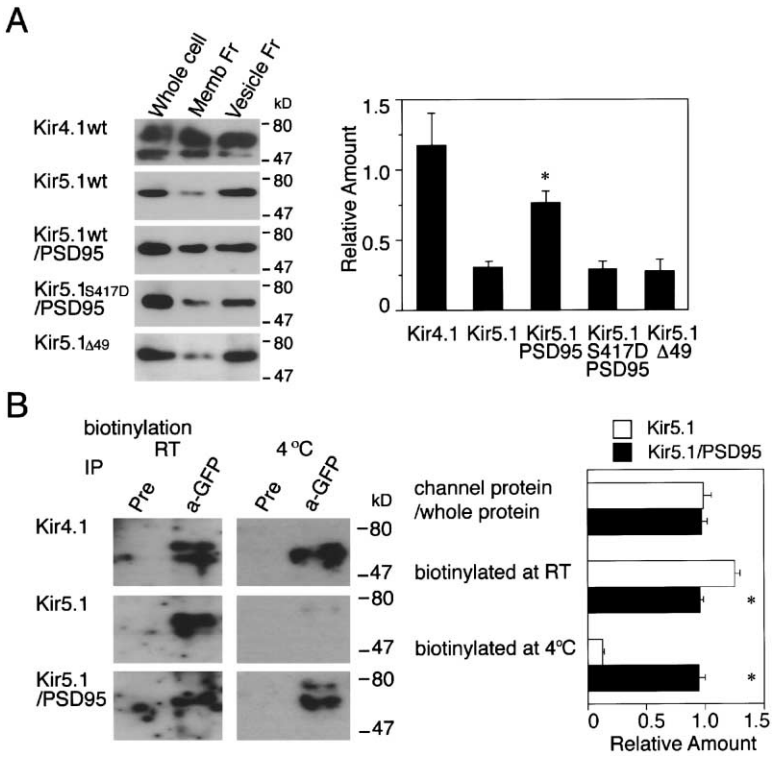

Figure 4. Effect of PSD-95 on the Intracellular Distribution of Kir5.1

(A) Increased membrane fraction expression of Kir5.1 by PSD-95 coexpression. The distribution of channel subunits, indicated at the left of each panel, was analyzed by sucrose gradient fractionation. A large amount of Kir4.1, which forms a functional channel by itself, existed in the membrane fraction. In contrast, little Kir5.1 expressed alone existed in the membrane fraction. Coexpression with PSD-95 increased the amount of Kir5.1 in the membrane fraction, but not that of Kir5.1S417D. Deletion of 49 C-terminal amino acids including an ER retention signal from Kir5.1 did not increase expression in the membrane fraction (Kir5.1Δ49). The bar graph summarizes the relative amounts of channel subunits in the membrane fraction compared to the vesicle fraction (means ± SE, n = 3). Asterisk indicates statistical significance between Kir5.1 and Kir5.1/PSD-95 ($p < 0.05$).

(B) Cell surface expression of Kir5.1. Channel subunits (indicated at the left of each panel) were surface biotinylated for 20 min at room temperature and 4°C. Immunoprecipitants with either preimmune control (Pre) or anti-GFP antibody (a-GFP) were detected by HRP-conjugated Streptavidin. A significant amount of each Kir channel subunit was biotinylated at room temperature (left panels). At 4°C, though Kir4.1 was biotinylated, little Kir5.1 was biotinylated. Coexpression with PSD-95 increased the amount of biotinylated Kir5.1 (right panels). The bar graph summarizes the relative amounts of Kir5.1 compared to Kir4.1 (means ± SE, n = 3). Asterisks indicate statistical significance between Kir5.1 and Kir5.1/PSD-95 ($p < 0.05$).

cell surface (i.e., the rate of sorting). In contrast, at 4°C, the amount of biotinylated Kir5.1 was much smaller when expressed alone (0.12 ± 0.04, n = 3) than when coexpressed with PSD-95 (0.94 ± 0.06, n = 3). These results suggest the following: (1) Kir5.1 expressed alone was synthesized and sorted to the plasma membrane but did not stay there, probably due to rapid internalization; (2) PSD-95 increased cell surface location of Kir5.1, not by increasing sorting, but probably by slowing internalization.

The intracellular movement of the Kir5.1 channel examined by the photobleaching technique supported the above notions (Figure 5). Excitation with extremely strong light makes GFP unable to emit fluorescence, a process known as bleaching. Thus, by examining the recovery after bleaching of GFP fluorescence tagged to Kir5.1 in certain areas of the cell, we could estimate the movement of GFP-Kir5.1 in the cell (Figures 5A and 5B). After bleaching the whole cell area (100%), GFP fluorescence recovered only slightly (<10%) within 10 min of observation. This indicates that little GFP-Kir5.1 protein was newly synthesized in this time scale.

When GFP-Kir5.1 was expressed alone, the fluorescence resumed gradually and reached a plateau within 2 min, regardless of the size of bleached areas (10%–90% of the cell area; Figure 5A). The relative intensity at plateau depended on the size of bleached area; i.e., when ~10%, 50%, 70%, or 90% of the whole cell area was bleached, the intensity in bleached regions recovered to ~60%, 35%, 30%, or 20% of the initial intensity, respectively. When PSD-95 was coexpressed with Kir5.1, the fluorescence at the bleached areas did not resume significantly within 10 min (Figure 5B). Even when only ~10% of whole cell area was bleached, the fluorescence recovered only to ~10% of the initial intensity. The profile in the fluorescence recovery of GFP-Kir5.1S417D coexpressed with PSD-95 was nearly identical to that of GFP-Kir5.1 expressed alone. These results clearly indicate that the sorting process of GFP-Kir5.1 expressed alone in HEK293T cells was rapid and that the protein relocated within several minutes. PSD-95 prominently slowed this relocation. If PSD-95 were to facilitate the sorting of Kir5.1, coexpression of PSD-95 should accelerate the relocation of GFP-Kir5.1, but this was not the case. Therefore, PSD-95 may not facilitate the insertion of Kir5.1, but may anchor Kir5.1 on the plasma membrane and slow its internalization, a conclusion that was further supported by the later experiments shown in Figure 7C.

Cotransfection of the minimal binding region of PSD-95 (PDZ3-SH3) to Kir5.1 did not alter the rate of relocation of Kir5.1 (Figure 5C). Thus, PDZ3-SH3 did not anchor Kir5.1 on the cell surface. This is probably the reason why PDZ3-SH3 could not produce a functional K^+ channel (Figure 3C). Based on this property of PDZ3-SH3, we examined the effect of PDZ3-SH3 on localization of Kir5.1 in cultured neurons (Figure 5D). PDZ3-SH3 was expressed in cultured neurons with the LipofectAMINE method. In 5 of 100 neurons examined, Kir5.1 immunoreactivity distributed diffusely within the cell (Figure 5D, lower panels). In contrast, in all mock-transfected neurons (n = 300), Kir5.1 immunoreactivity was detected on somato-dendritic regions in a clustered manner. Taking

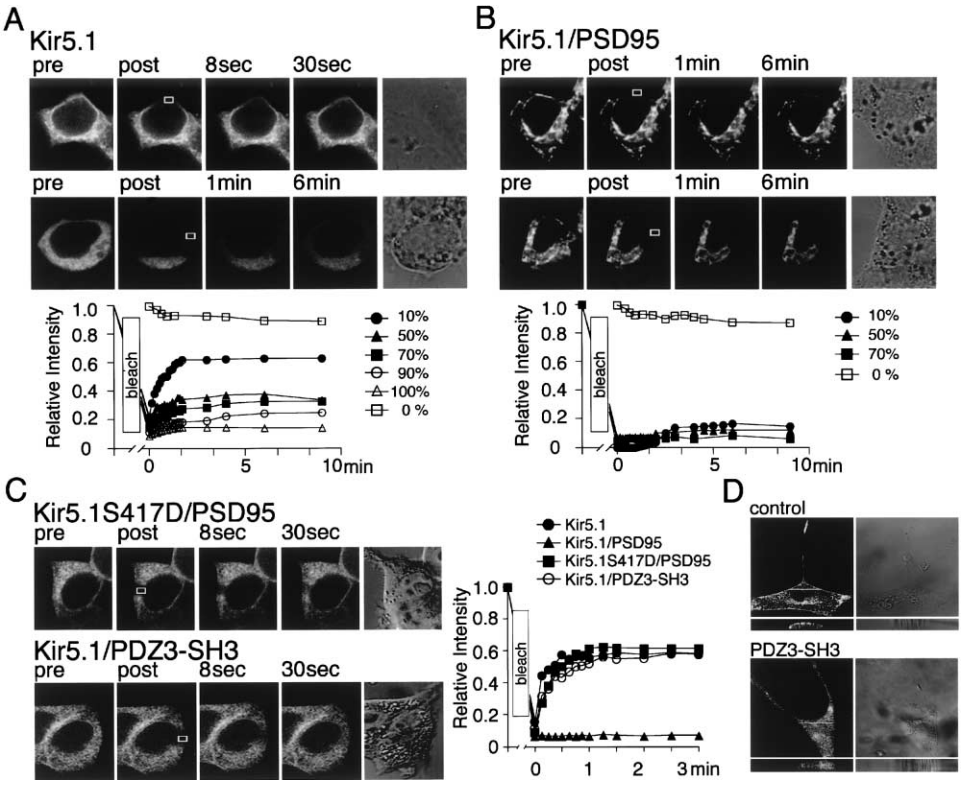

Figure 5. Effect of PSD-95 on the Intracellular Relocation of Kir5.1

(A and B) Diminished mobility of Kir5.1 by association with PSD-95. FRAP of GFP-Kir5.1 expressed alone (A) or with PSD-95 (B) in HEK293T cells. The time after bleaching is indicated above each panel. White squares indicate the area in which FRAP was counted (graphs). Sizes of bleached regions as a percentage of whole cell area are indicated by different symbols. When Kir5.1 was expressed alone, intensity recovered within several minutes. When Kir5.1 was coexpressed with PSD-95, intensity did not recover during the observation period of ~10 min.

(C) Effects of a point mutation (S417D) and a minimum binding domain of PSD-95 (PDZ3-SH3) on the mobility of Kir5.1. The rate of mobility of point mutant Kir5.1S417D coexpressed with full-length PSD-95 and wild-type Kir5.1 coexpressed with PDZ3-SH3 of PSD-95 was not changed compared to Kir5.1 expressed alone.

(D) Effects of PDZ3-SH3 overexpression on a cultured neuron. The upper and lower panels show top and side views of cells. White lines indicate the planes where side views are taken. Kir5.1 showed a clustered location near the plasma membrane in mock-transfected cells (control). Overexpression of PDZ3-SH3 induced diffuse distribution of Kir5.1 in the cytoplasm (PDZ3-SH3).

into account the low transfection efficiency of the LipofectAMINE method in primary cultured cells, this observation can be interpreted as indicating that overexpressed PDZ3-SH3 competed with intrinsic PSD-95 in binding to Kir5.1 and thus destroyed the somato-dendritic membrane localization of Kir5.1. Therefore, binding of intrinsic PSD-95 may be indispensable for clustered somato-dendritic distribution of Kir5.1 in neurons.

Effect of PKA Phosphorylation on Homomeric Kir5.1 Channel Activity

A point mutation, S417D, in Kir5.1 prevented Kir5.1/PSD-95 interaction (Figures 2E, 3A, 3C, and 4A). Because S417 is a putative PKA phosphorylation site and because the S417D mutation is supposed to mimic the phosphorylated state, PKA phosphorylation of S417 in Kir5.1 might disturb the interaction with PSD-95, as has been shown for Kir2.3 (Cohen et al., 1996).

In Kir5.1/PSD-95 cotransfected HEK293T cells, K^+ currents were elicited by a voltage step (500 ms in duration) from 0 to −100 mV every 6 s. When a solution containing 5 μM forskolin, 100 μM 8-Br-cAMP, and 100 μM IBMX (cAMP cocktail) was applied, K^+ currents were completely inhibited within 3 min (Figure 6A). After washing out the cAMP cocktail, K^+ currents recovered partially ($n = 5$). In the presence of 1 μM H89, the cAMP cocktail did not affect the K^+ currents ($n = 3$; data not shown). Because 1 μM H89 is a specific inhibitor of PKA (Chijiwa et al., 1990), it is possible that PKA phosphorylation is involved in Kir5.1/PSD-95 current inhibition.

We next examined the effects of cAMP treatment on Kir5.1/PSD-95 interaction in HEK293T cells (Figure 6B). In different conditions, immunoprecipitants with anti-PSD-95 antibody were obtained from the lysate of Kir5.1/PSD-95 cotransfected cells. PSD-95 interacted with Kir5.1 in control conditions, but cAMP treatment disrupted the interaction. Because 1 μM H89 prevented the effect of cAMP treatment, activation of PKA may be responsible for the disruption of the Kir5.1/PSD-95 complex. Kir5.1S417D was also not coimmunoprecipitated with PSD-95 (data not shown).

To examine if PKA activation disrupts Kir5.1/PSD-95 interaction in vivo, immunoprecipitation analysis with anti-Kir5.1 antibody from rat brain was performed (Figure 6C). While a significant amount of PSD-95 was de-

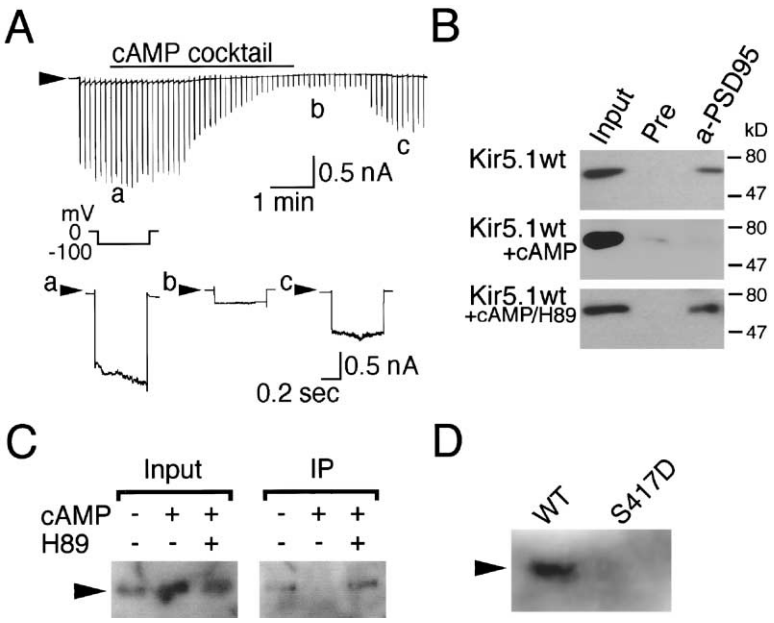

Figure 6. Effect of PKA Activation on Whole-Cell Current and Interaction of Kir5.1/PSD-95

(A) Suppression of Kir5.1/PSD-95 currents by PKA activation. A whole-cell current trace was recorded with voltage steps to −100 mV from a holding potential of 0 mV every 6 s. The cell was bathed in 140 mM $[K^+]_o$ solution. The solution with cAMP cocktail (5 μM forskolin, 100 μM 8-Br-cAMP, and 100 μM IBMX) was applied for the period indicated by the bar above the trace. cAMP treatment almost completely and reversibly reduced the current of Kir5.1/PSD-95.

(B) Disruption of the Kir5.1/PSD-95 complex by cAMP treatment. A lysate of Kir5.1/PSD-95-cotransfected HEK293T cells (Input) was immunoprecipitated with preimmune control (Pre) or anti-PSD-95 antibody (a-PSD95). Under control conditions (upper panel), Kir5.1 could bind to PSD-95. Binding was disrupted by a 10 min incubation with cAMP cocktail (middle panel), and this disruption was prevented by the inclusion of 1 μM of PKA-specific inhibitor H89 (lower panel).

(C) Disruption of Kir5.1/PSD-95 interaction by PKA activation in vivo in brain. Rat brain samples subjected to PKA activation/inhibition were immunoprecipitated with anti-Kir5.1 antibody, as described in Figure 1E. A lysate of each sample was loaded as a control (Input). The interaction of Kir5.1/PSD-95 was disrupted by PKA activation, and this disruption was inhibited by H89.

(D) PKA phosphorylation on CT58 of Kir5.1. Polyhistidine-tagged CT58 of Kir5.1 was subjected to PKA activation as described in (B), immunoprecipitated by anti-polyhistidine antibody, and detected by anti-phosphoserine antibody. The segment with the wild-type, but not S417 point-mutated, sequence was serine phosphorylated.

tected in the immunoprecipitant from the control preparation, no immunoreactivity was detected in that from the cAMP-pretreated preparation. In the presence of H89, the immunoprecipitant contained PSD-95 even after cAMP pretreatment. Because the content of proteins in the brain preparation was nearly the same among these experimental conditions, the disruption of Kir5.1/PSD-95 interaction by PKA activation may also occur in vivo.

The results so far showed that the disruption of the Kir5.1/PSD-95 interaction by PKA activation might be due to the phosphorylation of S417 in Kir5.1. In Figure 6D, therefore, we assessed the effect of cAMP treatment on the phosphorylation of serine residues in CT58 of Kir5.1. After cAMP treatment, the fragment containing the wild-type sequence of CT58, but not the one containing a mutation at S417, was detected by the antibody that specifically detects the phosphorylated form of serine residues. These results strongly support the notion that S417 of Kir5.1 is actually phosphorylated by cAMP treatment and suggest that this phosphorylation is responsible for PKA-mediated disruption of the Kir5.1/PSD-95 complex.

There are two possible ways by which PKA phosphorylation could suppress Kir5.1/PSD-95 current: (1) PKA phosphorylation of Kir5.1/PSD-95 directly affects the channel function itself; or (2) phosphorylation-induced separation of Kir5.1 and PSD-95 facilitates internalization of Kir5.1 and thus reduces the amount of Kir5.1 on the cell surface. To discriminate between these possibilities, we examined the localization of Kir5.1 in HEK293T cells during cAMP treatment (Figures 7A–7D).

The amounts of Kir5.1 in membrane and vesicle fractions of HEK293T cells cotransfected with PSD-95 were unaltered after 7 min cAMP treatment ($n = 3$; Figure 7A). The amount of Kir5.1 surface-biotinylated at both room temperature and 4°C was also unaffected after 10 min cAMP treatment (Figure 7B). The relative amount of Kir5.1 with reference to Kir4.1 was calculated by NIH image software. The content of Kir5.1 expressed in the cells was 0.97 ± 0.05 ($n = 3$) in the control (Figure 7B, "Pre") and 0.99 ± 0.06 ($n = 3$) after 10 min cAMP treatment (Figure 7B, "Post"). The amount of biotinylated Kir5.1 at room temperature was 0.95 ± 0.04 (Figure 7B, "Pre") and 0.94 ± 0.06 (Figure 7B, "Post"), and that at 4°C was 0.94 ± 0.06 (Figure 7B, "Pre") and 0.93 ± 0.16 (Figure 7B, "Post") ($n = 3$ for each).

In Figure 7C, the alteration in fluorescence intensity of GFP-Kir5.1 in the vicinity of the cell surface was compared with and without cAMP treatment. In HEK293T cells expressing GFP-Kir5.1, most of the cell area was bleached out, and the fluorescence of the small, unbleached areas in the vicinity of the cell surface was monitored. In the cells expressing GFP-Kir5.1 alone (Figure 7C, upper panels), the intensity reduced rapidly within several minutes and reached ~25% and ~15% of the initial value after 10 and 40 min of monitoring, respectively (closed circles in the right graph in Figure 7C). When PSD-95 was coexpressed, the rate of reduction was very slow; the intensity was about 70% and 50% of the initial value after 10 and 40 min, respectively (Figure 7C, closed triangles). The cAMP treatment of cells did not significantly alter the time course up to 10 min. During cAMP treatment longer than 10 min, the fluorescence faded faster than the time course without cAMP treatment; only ~25% of the initial value remained after 40 min of treatment (Figure 7C, lower panels and closed squares in the graph). The speed of relocation

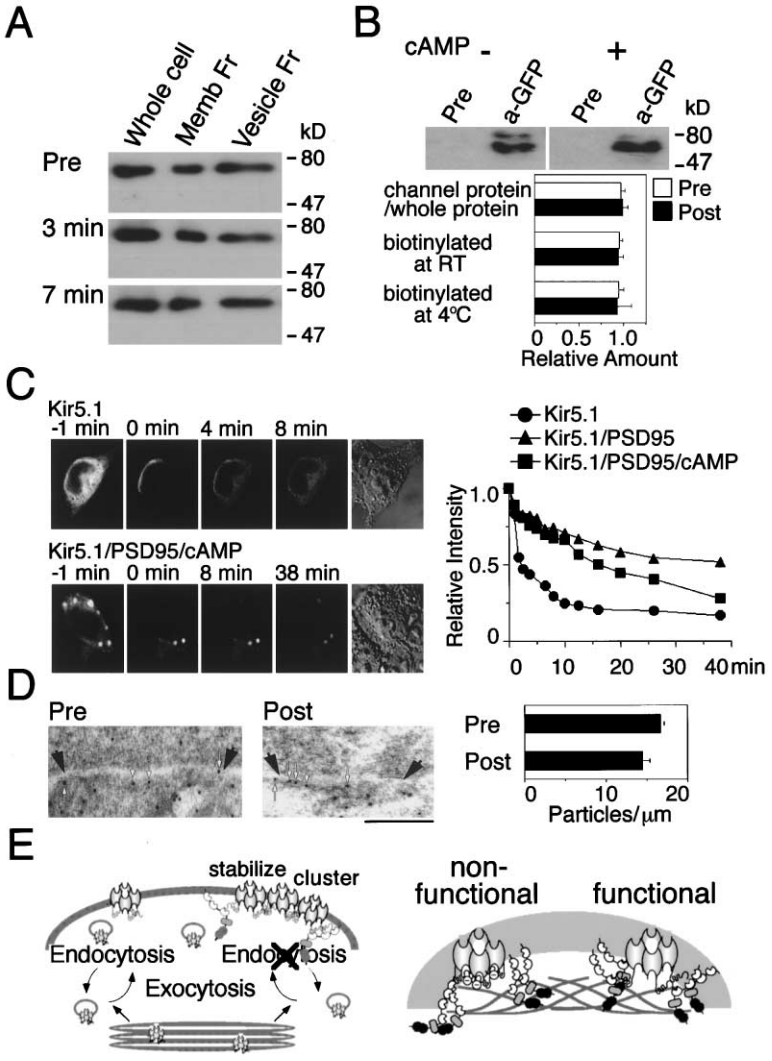

Figure 7. Effect of PKA Activation on Kir5.1 Location

(A) Intracellular distribution of Kir5.1 during cAMP treatment. The intracellular distribution of Kir5.1 was examined, as described in Figure 4A, during cAMP treatment (the incubation periods are indicated at the left of each panel). The distribution of Kir5.1 did not change.

(B) Cell-surface expression of Kir5.1 during cAMP treatment. Kir5.1/PSD-95-cotransfected cells were cell surface biotinylated without (−, Pre) or with (+, Post) cAMP cocktail treatment and examined as described in Figure 4B (graph). The upper panels show the result of biotinylation at 4°C. The amount of biotinylated Kir5.1 was not changed by a 10 min cAMP treatment, either at room temperature or at 4°C (graph).

(C) Mobility of Kir5.1 during cAMP treatment. Without PSD-95, coexpression fluorescence in the unbleached area diffused (Kir5.1). PSD-95 coexpression reduced the rate of diffusion, even under cAMP treatment (Kir5.1/PSD95/cAMP). This rate was almost same as that without cAMP treatment up to 10 min (graph), but was faster during longer treatment. The duration after bleaching is indicated above each panel.

(D) Electron microscopic observations of Kir5.1/PSD-95 before and after cAMP treatment. The density of particles adjacent to the cell surface was counted before (Pre) and after 10 min (Post) a cAMP treatment, as described in Figure 2C. No significant reduction of cell surface immunoreactivity was observed. Scale bar: 300 nm.

(E) Schematic model for PSD-95 to form functional Kir5.1. PSD-95 plays dual roles to form functional Kir5.1: (1) anchoring Kir5.1 on the cell surface and (2) making surface Kir5.1 functional. Kir5.1 is continuously transported to the cell surface, but is rapidly internalized without forming a functional channel. PSD-95 anchors and clusters Kir5.1 on the cell surface by interacting with its C terminus (left). The cluster probably contains several intracellular components, including cytoskeleton, and Kir5.1 is not internalized rapidly, even after disruption of its interaction with PSD-95. Kir5.1 cannot form functional channels without the interaction with PSD-95, even when channels exist on the cell surface. PSD-95 makes Kir5.1 functional, probably through interaction with the C terminus of Kir5.1 (right).

in this condition, however, was still slower than that of Kir5.1 expressed alone. Furthermore, by immunoelectron microscopic examination, it was confirmed that the density of gold particles for GFP-Kir5.1 immunoreactivity in the vicinity of plasma membrane was similar before and after a 10 min cAMP treatment (Figure 7D). The density of particles was 16.64 ± 0.96/μm and 14.40 ± 1.20/μm (n = 3 for each) before and after cAMP treatment, respectively (graph in Figure 7D). These results may indicate that cAMP treatment did not significantly affect either the sorting or retrieval rate of Kir5.1 from the cell surface in cells cotransfected with PSD-95 during the initial 10 min enough to suppress channel activity. Although binding of PSD-95 is mandatory to form clusters of Kir5.1 on cell surface, it seems likely that once incorporated in the clusters, unbinding of Kir5.1 from PSD-95 caused not rapid but slow internalization of Kir5.1, requiring more than 10 min. Thus, because PKA phosphorylation of Kir5.1 caused Kir5.1/PSD-95 current inhibition within 3 min, the direct effect of phosphorylation on the function of the Kir5.1/PSD-95 channel, but not facilitation of channel internalization, may cause this inhibition (Figure 7E).

Discussion

This study shows that Kir5.1 subunits can form functional homomeric K^+ channels by interacting with PSD-95. Several other members of the Kir family, including Kir3.0 and Kir6.0, are also nonfunctional when expressed alone (Inagaki et al., 1995; Inanobe et al., 1999). Because Kir channels play critical roles in the control of cell excitability, it is important to examine how these "mute" Kir subunits can be functional in situ. Heteromeric assemblies with other proteins have been reported to make these "mute" subunits functional. For example, the Kir3.0 subfamily forms heteromeric assemblies with other members of this subfamily (Inanobe et

al., 1999). The Kir6.0 subfamily associates with entirely different membrane proteins, sulfonylurea receptors (SURs) (Inagaki et al., 1995). In this study, we show that another family of proteins, MAGUKs, are necessary to form a functional channel from the homomeric assembly of Kir5.1 subunits. (Figure 7E).

In the hetero-octameric assemblies of Kir6.2 and SURs, the ER retention signals, RKR or RRR, which exist in both components, are concealed, and the complex can then be sorted to plasma membrane (Zerangue et al., 1999). By deletion of this retention signal, Kir6.2 can form a functional ATP-sensitive K^+ channel on the plasma membrane (Tucker et al., 1997). Thus, in the case of Kir6.2, one role of SURs is to prevent retention in ER and aid the sorting of the Kir subunit to the plasma membrane. The retention signal, RRR, in the C terminus of Kir5.1, on the other hand, did not play a significant role. This study showed that while Kir5.1 expressed alone in HEK293T cells was under rapid exocytotic-endocytotic turnover, PSD-95 stabilized Kir5.1 on the plasma membrane, not by facilitating insertion, but by preventing internalization.

PKA phosphorylation inhibited the activity of the Kir5.1/PSD-95 channel within several minutes. Although the relocation of Kir5.1 coexpressed with PSD-95 was facilitated to some extent by cAMP treatment, the speed was still slow, and Kir5.1 remained in the clusters at least during the initial 10 min of treatment. Therefore, the internalization of channel proteins could not account for the PKA-induced inhibition of Kir5.1 channel activity. This was unexpected, because PSD-95 was needed to form clusters of Kir5.1 stabilized on the cell surface. The mechanism was unclear about how Kir5.1 remained almost constant on the cell surface around 10 min, even after PKA-mediated disruption of the interaction with PSD-95. PSD-95 is, however, known to interact, not only with membrane proteins, but also with various intracellular proteins such as CRIPT and SPAR (Niethammer et al., 1998; Sheng, 2001). Therefore, it is expected that the clusters of Kir5.1 and PSD-95 may contain various proteins, including tubulin-based and actin-based cytoskeletons (Craven and Bredt, 1998; Sheng, 2001). These cytoskeletal proteins might provide some additional mechanisms for stabilization of Kir5.1 on the cell surface, which may slow down the internalization of Kir5.1 even after disruption of binding with PSD-95. The reduction of the Kir5.1/PSD-95 current by PKA without affecting clustered distribution of Kir5.1 might explain why only about half of Kir5.1/PSD-95 coexpressing cells showed K^+ channel activity. In those cells that exhibited no K^+ current despite the clustered distribution, the Kir5.1/PSD-95 complex might have been PKA phosphorylated and become nonfunctional.

There are two possible mechanisms for the PKA-mediated inhibition of the Kir5.1/PSD-95 channel function itself. First, unbinding of PSD-95 from Kir5.1 diminishes channel function. Interaction with MAGUKs also influences the function of other Kir channels; SAP97 confers G protein sensitivity to Kir3.2c (Hibino et al., 2000), and interaction with PSD-95 affects the activity of Kir2.3 (Nehring et al., 2000). Therefore, it is possible that MAGUKs may directly regulate the channel function of Kir5.1. Second, phosphorylation of Kir5.1 itself may inhibit channel activity. It was reported, for example, that PKA-mediated phosphorylation causes suppression of Kir2.1 channel activity (Wischmeyer and Karschin, 1996). In *Xenopus* oocytes, it was reported that Kir5.1 subunits expressed alone locate on the cell surface but do not show K^+ channel activity (Salvatore et al., 1999). One possibility would be that Kir5.1 channels might have been phosphorylated in oocytes, which contain a higher concentration of cAMP than mammalian cells, and thus did not show K^+ channel activity. However, in Kir5.1-expressing oocytes, we could not detect any additional K^+ currents, even following treatment with H89, a specific PKA inhibitor ($n = 5$; our unpublished data). In HEK293T cells, some small but significant fraction of Kir5.1 was expressed on the cell surface even in the absence of PSD-95. But these channels did not show any detectable K^+ channel activity. Therefore, the first, but not the second, possibility seems to be more likely. Recently, it has been reported that the chloride channel activity of CFTR is enhanced by an accessory protein, CAP70 (Wang et al., 2000). It is postulated that CAP70 may play a role in assembling and changing the array of CFTR subunits. Similarly, PSD-95 might change the array and conformation of Kir5.1 channels through interaction with the C terminus of Kir5.1 (Figure 7E, right panel). This study showed that Kir5.1/PSD-95 interaction was disrupted by PKA activation or a phosphorylation-mimic mutation of S417 (S417D) in Kir5.1. Because CT58 of Kir5.1 was enough to interact with PSD-95 and only S417 seemed to be PKA phosphorylated in this segment, PKA phosphorylation of the S417 residue in Kir5.1 might be responsible for the disruption of the interaction and thus decrease channel activity. Further studies are, however, needed to clarify how PSD-95 controls channel activity.

For binding to PSD-95, Kir5.1 exhibited a unique property. While most ion channels and receptors so far reported to interact with MAGUKs (glutamate receptors, $K_V1.0$, and Kir2.3) bind to PDZ1 and/or PDZ2 domains of PSD-95 (Kim et al., 1995; Kornau et al., 1995; Cohen et al., 1996), Kir5.1 bound to the region from PDZ3 to SH3. Containing Q and R at the -1 and -7 position from the carboxyl end, which fulfills the binding property for PDZ3 of PSD-95, the carboxyl tail of Kir5.1 would interact with PDZ3 of PSD-95 (Niethammer et al., 1998). For this interaction, the SH3 domain of PSD-95 may also play some role. Because SH3 domains of several proteins are implicated in the endocytic process through clathrin-coated vesicle formation (Simpson et al., 1999), the SH3 domain of PSD-95 might be involved in PSD-95-induced slowing down of Kir5.1 internalization.

The Kir5.1/PSD-95 complex was actually detected on somato-dendritic plasma membrane in primary cultured neurons, and the activity of the Kir5.1/PSD-95 channel was reversibly inhibited by PKA activation in HEK293T cells. MAGUKs, including PSD-95, are reported to function as scaffolds for PKA-mediated signal molecules, such as PKA and phosphatases, and may facilitate PKA-mediated neuronal regulation (Colledge et al., 2000; Westphal et al., 1999). Thus, it is possible that the Kir5.1/PSD-95 complex may exist at the PSD of dendritic spines in vivo and play an important functional role in synaptic transmission. Functional Kir5.1/PSD-95 channels at PSD may induce hyperpolarization of dendritic spines, which can be effectively depolarized by activa-

tion of PKA at the PSD. This depolarization may facilitate the action of glutamate receptors. This might explain, at least in part, the means by which PKA facilitates neuronal excitability (Fraser and Scott, 1999). Therefore, the Kir5.1/PSD-95 channel complex is potentially a novel physiological target of PKA-mediated signals at the PSD of excitatory synapses. Further studies, however, are needed to clarify the physiological roles of Kir5.1/PSD-95 in brain.

Experimental Procedures

Expression of Kir4.1, Kir5.1, and PSD-95

Wild-type and mutant GFP-tagged rat Kirs were constructed by subcloning each coding region into a mammalian cell expression vector, pEGFP-C1 (CLONTECH Laboratories, Palo Alto, CA). Rat PSD-95 cDNA was a gift from Dr. Takai. These plasmid vectors were transfected into a human embryonic kidney cell line, HEK293T, by using LipofectAMINE (Life Technologies, Gaitheresburg, MD) according to the manufacturer's instructions. For the experiments of PSD-95 coexpression, three times more PSD-95 cDNA was cotransfected with each Kir5.1 cDNA. Electrophysiological and biochemical analyses were usually conducted 2–4 days after transfection.

Electrophysiological Recordings

Channels expressed in HEK293T cells were analyzed with a patch clamp method in whole-cell configurations as reported previously (Tanemoto et al., 2000). All experiments were performed at room temperature (22°C–24°C). The pipette solution contained 140 mM KCl, 1 mM $MgCl_2$, 1 mM $CaCl_2$, and 5 mM HEPES-KOH (pH 7.4). The bath solution contained 140 mM KCl, 5 mM EGTA, 2 mM $MgCl_2$, and 5 mM HEPES-KOH (pH 7.3). In experiments with different $[K^+]_o$ conditions, K^+ in the bath solution was substituted with Na^+.

Antibodies

Affinity purified polyclonal anti-Kir5.1 antibody was prepared as reported previously (Tanemoto et al., 2000). A rabbit polyclonal anti-PSD-95 antibody was a gift from Dr. Takai. Mouse monoclonal anti-dlg/SAP97, anti-PSD-95 (Transduction Laboratories, Lexington, KY), anti-polyhistidine, anti-phosphoserine (Sigma, St. Louis, MO), and anti-GFP and rabbit polyclonal antibodies (CLONTECH) were commercially obtained.

Confocal and Electron Microscopy

Cerebral neuron cultures were performed from E17–E18 rat embryos dissociated with trypsin and plated on coverslips coated with poly-L lysine in DMEM containing 20% fetal calf serum.

Cultured neurons and HEK293T cells were fixed, and immunofluorescence observation was performed as previously described (Inanobe et al., 1999). For the experiment with photo-bleaching and cAMP cocktail application, cells were directly observed in the bath solution. Photobleaching was performed by exciting GFP-tagged channel proteins in certain area of cells with extremely strong light of 485 nm wavelength. Confocal microscopic observation was performed on a model LSM510 (Carl Zeiss, Jena, Germany).

Immunogold electron microscopic observation was performed as described previously (Hibino et al., 2000).

Subcellular Fractionation

Cell homogenates were crudely fractionated in solution containing 0.25 M sucrose, 25 mM EDTA, and 0.05 M Tris (pH 7.4) by gravity. In brief, homogenates were centrifuged under the gravity of 300 × g. The supernatant was further centrifuged under the gravity of 10,000 × g and then 200,000 × g, and precipitants were collected as a membrane fraction and a vesicle fraction, respectively. Each fraction was solubilized in triple detergent lysis buffer (50 mM Tris-HCl [pH 7.4], 150 mM NaCl, 1 μg/ml aprotinin, 100 μg/ml phenylmethylsulfonyl fluoride (PMSF), 0.02% NaN_3, 1% Triton X-100, 0.1% SDS, and 0.5% sodium deoxycholate). About 10 μg of solubilized protein from each fraction was analyzed.

Immunoblot and Immunoprecipitaiton Analyses

An adult male Spraque-Dawley rat was anesthesized and killed according to the regulations of the Animal Care Committee of Osaka University. Preparation of transfected HEK293T cells and rat brain and immunoprecipitation were performed and analyzed as previously described (Tanemoto et al., 2000). The intensity of detected proteins was calculated using NIH Image software (National Institutes of Health, Bethesda, MD).

GST Pull-Down Analysis

Glutathione S transferase (GST) fusion proteins of specific regions of Kir5.1 and PSD-95 were constructed by subcloning PCR-amplified DNA fragments into the bacterial expression vector pGEX-5X3 (Amersham Pharmacia Biotech, Uppsale, Sweden). GST-fusion proteins contained the following regions of each protein: Kir5.1CT: wt (362–419), ΔSQM (362–416), S417D (362–419 with S417 changed to D); PSD95: Full (1–725), PDZ1-GK (64–725), PDZ2-GK (159–725), PDZ3-GK (312–725), SH3-GK (436–725), NT-SH3 (1–495), PDZ2-SH3 (159–495), PDZ3-SH3 (312–495), PDZ1-2-3 (1–393), PDZ3 (312–393), ΔPDZ3 (1–311 and 394–725), ΔSH3 (1–435 and 496–725). Pull-down studies were performed as previously described (Hibino et al., 2000).

PKA Phosphorylation

Experiments with PKA stimulation were performed using cAMP cocktail containing 5 μM forskolin, 100 μM 8-Br-cAMP, and 100 μM IBMX. In immunoprecipitation and cell surface biotinylation analyses, cAMP cocktail was applied for 10 min until just before further preparation. For inhibition of PKA phosphorylation, PKA-specific blocker N-(2([3-(4-bromophenyl)-2-propenyl]amino)-ethyl)-5-isoquinolinesulfonamide (H89) (Seikagaku, Tokyo, Japan) was applied for 3 min before and during application of cAMP cocktail at a concentration of 1 μM. For the experiment of Kir5.1 C-terminal phosphorylation, polyhistidine-tagged C-terminal Kir5.1s (362–419 and 362–419 with S417 changed to D) was constructed by subcloning PCR-amplified DNA fragments into the expression vector pcDNA4/HisMaxC (Invitrogen, Carlsbad, CA).

Cell Surface Biotinylation

Transfected cells were washed with ice-cold phosphate buffer (PB) (pH 7.4) containing 120 mM NaCl, 4.4 mM KH_2PO_4, and 20.6 mM Na_2HPO_4. Then, cell surface proteins were biotinylated with 2 mg/ml Sulfo-NHS LC-Biotin (Pierce, Rockford, IL) in PB for 20 min at room temperature or 4°C. Unreacted biotin reagent was blocked by the addition of an equal volume of 10 mM glycine in PB for >10 min at room temperature, followed by three washes with ice-cold PB. Immunoprecipitation analysis was performed as described above using anti-GFP antibody, and immunoprecipitants were analyzed by Western blotting using Streptavidin-biotinylated horseradish peroxidase (HRP) complex (Amersham Pharmacia Biotech).

Acknowledgments

We thank Dr. Ian Findlay for his critical comments on this manuscript. This work was supported by the Grant-in-Aid for Specific Research on Priority Area (B) (12144207) (Y.K.) and by the Grant-in-Aid for Encouragement of Young Scientists (13770599) (M.T.) from the Ministry of Education, Science, Sports and Culture of Japan, and by a grant from the Research for the Future Program of the Japanese Society for the Promotion of Science (96L00302) (Y.K.).

Received: July 24, 2001
Revised: February 21, 2002

References

Bond, C.T., Pessia, M., Xia, X.M., Lagrutta, A., Kavanaugh, M.P., and Adelman, J.P. (1994). Cloning and expression of a family of inward rectifier potassium channels. Receptors Channels *2*, 183–191.

Chijiwa, T., Mishima, A., Hagiwara, M., Sano, M., Hayashi, K., Inoue, T., Naito, K., Toshioka, T., and Hidaka, H. (1990). Inhibition of forskolin-induced neurite outgrowth and protein phosphorylation by a newly synthesized selective inhibitor of cyclic AMP-dependent

protein kinase, N-[2-(p-bromocinnamylamino)ethyl]-5-isoquinolinesulfonamide (H-89), of PC12D pheochromocytoma cells. J. Biol. Chem. *265*, 5267–5272.

Cho, K.-O., Hunt, C.A., and Kennedy, M.B. (1992). The rat brain postsynaptic density fraction contains a homolog of the drosphila discs-large tumor suppressor protein. Neuron *9*, 929–942.

Cohen, N.A., Brenman, J.E., Snyder, S.H., and Bredt, D.S. (1996). Binding of the inward rectifier K+ channel Kir 2.3 to PSD-95 is regulated by protein kinase A phosphorylation. Neuron *17*, 759–767.

Colledge, M., Dean, R.A., Scott, G.K., Langeberg, L.K., Huganir, R.L., and Scott, J.D. (2000). Targeting of PKA to glutamate receptors through a MAGUK-AKAP complex. Neuron *27*, 107–119.

Craven, S.E., and Bredt, D.S. (1998). PDZ proteins organize synaptic signaling pathways. Cell *93*, 495–498.

Fraser, I.D., and Scott, J.D. (1999). Modulation of ion channels: a current view of AKAPs. Neuron *23*, 423–426.

Hibino, H., Inanobe, A., Tanemoto, M., Fujita, A., Doi, K., Kubo, T., Hata, Y., Takai, Y., and Kurachi, Y. (2000). Anchoring proteins confer G protein sensitivity to an inward-rectifier K(+) channel through the GK domain. EMBO J. *19*, 78–83.

Inagaki, N., Gonoi, T., Clement, J.P., IV, Namba, N., Inazawa, J., Gonzalez, G., Aguilar-Bryan, L., Seino, S., and Bryan, J. (1995). Reconstitution of IKATP: an inward rectifier subunit plus the sulfonylurea receptor. Science *270,* 1166–1170.

Inanobe, A., Yoshimoto, Y., Horio, Y., Morishige, K.I., Hibino, H., Matsumoto, S., Tokunaga, Y., Maeda, T., Hata, Y., Takai, Y., and Kurachi, Y. (1999). Characterization of G-protein-gated K+ channels composed of Kir3.2 subunits in dopaminergic neurons of the substantia nigra. J. Neurosci. *19*, 1006–1017.

Isomoto, S., Kondo, C., and Kurachi, Y. (1997). Inwardly rectifying potassium channels: their molecular heterogeneity and function. Jpn. J. Physiol. *47*, 11–39.

Jan, L.Y., and Jan, Y.N. (1997). Cloned potassium channels from eukaryotes and prokaryotes. Annu. Rev. Neurosci. *20*, 91–123.

Kim, E., Niethammer, M., Rothschild, A., Jan, Y.N., and Sheng, M. (1995). Clustering of Shaker-type K+ channels by interaction with a family of membrane-associated guanylate kinases. Nature *378*, 85–88.

Kornau, H.C., Schenker, L.T., Kennedy, M.B., and Seeburg, P.H. (1995). Domain interaction between NMDA receptor subunits and the postsynaptic density protein PSD-95. Science *269*, 1737–1740.

Nehring, R.B., Wischmeyer, E., Doring, F., Veh, R.W., Sheng, M., and Karschin, A. (2000). Neuronal inwardly rectifying K(+) channels differentially couple to PDZ proteins of the PSD-95/SAP90 family. J. Neurosci. *20*, 156–162.

Niethammer, M., Valtschanoff, J.G., Kapoor, T.M., Allison, D.W., Weinberg, T.M., Craig, A.M., and Sheng, M. (1998). CRIPT, a novel postsynaptic protein that binds to the third PDZ domain of PSD-95/SAP90. Neuron *20*, 693–707.

Pearson, W.L., Dourado, M., Schreiber, M., Salkoff, L., and Nichols, C.G. (1999). Expression of a functional Kir4 family inward rectifier K+ channel from a gene cloned from mouse liver. J. Physiol. (Lond.) *514*, 639–653.

Pessia, M., Tucker, S.J., Lee, K., Bond, C.T., and Adelman, J.P. (1996). Subunit positional effects revealed by novel heteromeric inwardly rectifying K+ channels. EMBO J. *15*, 2980–2987.

Salvatore, L., D'Adamo, M.C., Polishchuk, R., Salmona, M., and Pessia, M. (1999). Localization and age-dependent expression of the inward rectifier K+ channel subunit Kir5.1 in a mammalian reproductive system. FEBS Lett. *449*, 146–152.

Sheng, M. (2001). Molecular organization of postsynaptic specialization. Proc. Natl. Acad. Sci. USA *98*, 7058–7061.

Simpson, F., Hussain, N.K., Qualmann, B., Kelly, R.B., Kay, B.K., McPherson, P.S., and Schmid, S.L. (1999). SH3-domain-containing proteins function at distinct steps in clathrin-coated vesicle formation. Nat. Cell Biol. *1*, 119–124.

Tanemoto, M., Kittaka, N., Inanobe, A., and Kurachi, Y. (2000). In vivo formation of a proton-sensitive K+ channel by heteromeric subunit assembly of Kir5.1 with Kir4.1. J. Physiol. (Lond.) *525*, 587–592.

Tucker, S.J., Gribble, F.M., Zhao, C., Trapp, S., and Ashcroft, F.M. (1997). Truncation of Kir6.2 produces ATP-sensitive K+ channels in the absence of the sulphonylurea receptor. Nature *387*, 179–183.

Tucker, S.J., Imbrici, P., Salvatore, L., D'Adamo, M.C., and Pessia, M. (2000). pH dependence of the inwardly rectifying potassium channel, Kir5.1, and localization in renal tubular epithelia. J. Biol. Chem. *275*, 16404–16407.

Wang, S., Yue, H., Derin, R.B., Guggino, W.B., and Li, M. (2000). Accessory protein facilitated CFTR-CFTR interaction, a molecular mechanism to potentiate the chloride channel activity. Cell *103*, 169–179.

Westphal, R.S., Tavalin, S.J., Lin, J.W., Alto, N.M., Fraser, I.D., Langeberg, L.K., Sheng, M., and Scott, J.D. (1999). Regulation of NMDA receptors by an associated phosphatase-kinase signaling complex. Science *285*, 93–96.

Wischmeyer, E., and Karschin, A. (1996). Receptor stimulation causes slow inhibition of IRK1 inwardly rectifying K+ channels by direct protein kinase A-mediated phosphorylation. Proc. Natl. Acad. Sci. USA *93*, 5819–5823.

Xu, H., Cui, N., Yang, Z., Qu, Z., and Jiang, C. (2000). Modulation of Kir4.1 and Kir5.1 by hypercapnia and intracellular acidosis. J. Physiol. (Lond.) *3*, 725–735.

Zerangue, N., Schwappach, B., Jan, Y.N., and Jan, L.Y. (1999). A new ER trafficking signal regulates the subunit stoichiometry of plasma membrane K(ATP) channels. Neuron *22*, 537–548.